

We are IntechOpen, the world's leading publisher of Open Access books Built by scientists, for scientists

6,900

Open access books available

185,000

International authors and editors

200M

Downloads

Our authors are among the

154

Countries delivered to

TOP 1%

most cited scientists

12.2%

Contributors from top 500 universities



WEB OF SCIENCE™

Selection of our books indexed in the Book Citation Index
in Web of Science™ Core Collection (BKCI)

Interested in publishing with us?
Contact book.department@intechopen.com

Numbers displayed above are based on latest data collected.
For more information visit www.intechopen.com



Use of Microfluidic Technology for Cell Separation

Hisham Mohamed

Additional information is available at the end of the chapter

<http://dx.doi.org/10.5772/50382>

1. Introduction

1.1. Motivation for cell sorting

The cell is the basic functional unit within a tissue or an organ. Methods that can be used to probe the cell, so as to understand, or even manipulate its interrelated processes, pathways, and/or overall functioning, are of great scientific and commercial value. Research efforts in molecular biology, biochemistry, and biotechnology over the last two decades have created high demand for efficient, cost-effective, cell enrichment, isolation, and handling methods. Cell studies can be performed on continuously growing cell lines, many of which are commercially available, in tissue culture, or on cells obtained from intact tissues or isolated from blood [1-3].

Mammalian cells are highly heterogeneous in structure, function, and characteristics. However, many types of biochemical, pharmaceutical, and clinical studies, such as immunophenotyping, studies of the cell cycle, cell proliferation, or apoptosis, and other specialized cell analyses require a homogenous population consisting of a single cell type; as the analyte. Only then can the results be deemed accurate and specific to the cell type under investigation [4, 5]. Accordingly, techniques to separate cell types in a heterogeneous cell population are of immense practical value. Any such efforts are further complicated when the target cell is rare within a population such as in many cancer and prenatal diagnosis applications. The more stringent the requirements for specific and precise cell separation, the greater the degree of accuracy and reproducibility required in the technology that underlies the separation method [6-8].

Recent progress in microfabrication, technologies developed and utilized by the integrated circuits (ICs) industry, is being exploited to biomedicine, spawning a relatively new field of research that has become known as BioMEMS. Microfabricated devices have already had a

broad range of biomedical and biological applications [9, 10]. These devices can be manufactured with a reproducible accuracy of less than 1 micrometer (1/100th the diameter of a human hair). In the last decade, microchips have been used in a huge range of devices and contexts: microscale sensors for surgical instruments, monitoring of physiological activities, drug discovery and delivery, DNA amplification, and electrophoresis, as well as cell sorting, the application discussed in this chapter [11-16].

Microfluidic technology, a subcategory of BioMEMS, is a set of techniques and processes for making devices to precisely control and manipulate fluid in a geometrically small channels; sub- to few hundred- micrometers in size. Microfluidic is multi-disciplinary; developing a device with biological utility requires the integration of knowledge and techniques from the fields of engineering, biology, physics, and chemistry. Such microfabricated devices are used to study biological systems and to generate new insights into how these systems work. Conversely, the biological knowledge gained through micro/nano - scale analyses can lead to further improvements in device design. BioMEMS is a challenging field because the materials, and chemistries, important for biological microfluidics applications are so diverse [17, 18].

The objective of the present chapter is to introduce the principals of cell sorting by microfluidic technology, and to discuss its strengths, current limitations, and current and potential applications, with illustrative examples from the literature and from the author's laboratory.

1.2. Challenges in cell sorting

Cells of different types have characteristic sizes, shapes, densities, and arrays of surface molecules that can be exploited for sorting. For example, red blood cells (RBCs) are the cells responsible for delivering oxygen to the tissues. RBCs have to squeeze through capillaries and therefore are relatively small, approximately 6-8 μm in diameter, and flexible. Mature RBCs are anucleate; the maturing cells lose their nuclei before leaving the bone marrow. Loss of the nucleus leads to cell membrane collapse, conferring the characteristic biconcave shape of RBCs, and giving the cell a greater surface area to volume ratio than of spherical cells. These physical features allow easier movement of oxygen (O_2) and carbon dioxide (CO_2) through the membrane. RBCs are composed mainly of hemoglobin, whose iron atoms temporarily bind O_2 molecules in the lungs, and then release the molecules throughout the body. RBCs have the highest density of any cell type in blood. All of the above characteristics can be used for separation: for example size can be used to separate RBCs since they are smaller and more flexible than white blood cells (WBCs). RBCs' high density causes them to spin down to the bottom of a test tube after density gradient centrifugation. The high iron content gives RBCs intrinsic magnetic properties and can be used for magnetic separation [19].

In other cases, a cell changes its shape or size as a result to a disease or change in function. In sickle-cell disease, a genetic blood disorder, RBCs assume an abnormal, rigid, sickle

shape. The change in shape and the increased rigidity of the RBCs lead to obstruction of capillaries, thereby restricting blood flow to organs, causing anemia and other “sickle cell crisis”, and decreasing life expectancy. Cancer is a second example of such changes [20]. Malignant tumor cells differ from benign tumor cells in structure, growth rate, invasiveness, and their ability to metastasize. Benign tumor cells grow slowly, pushing neighboring tissues away while staying well encapsulated. In contrast, malignant tumor cells grow rapidly, invade neighboring tissues, and may metastasize [21]. Furthermore, they generally are irregular in shape, and exhibit a more “rugged” or “ruffled” surface appearance than do normal cells [22, 23]. Cancer is detected and diagnosed based on physical changes present in tissues and cells. Nuclear changes such as an increase in size, deformation, and a change in internal organization are among the most universal criteria for detecting malignancy [24-25]. These changes may reflect alterations in the nuclear matrix and the connections of the nuclear matrix to or via the cytoskeleton. Cancer cells modify their morphology, principally by increasing the size of the nucleus, before they become invasive, i.e., in dysplasia and carcinoma *in situ*. The nucleus of a dysplastic cell can be up to four times as large as that of a non-dysplastic cell. Accordingly, light scattering microscopy has been used to distinguish normal, dysplastic, and cancerous epithelial cells in a range of tissues including esophagus, colon, bladder, and oral cavity [26]. However, this technique can only succeed if a sufficient number of cells are available for analysis.

Additionally, most cell types have characteristic complements of surface molecules. Among the most useful for identification is the cluster of differentiation (CD), or cluster of designation. CD molecules have roles in signaling and adhesion processes, and the specific complements of CD molecules is a determinant of the specific function of the cell. Cell populations are usually denoted by a pattern of “+” or a “-” scorings; indicating the presence or absence of specific CD molecules. For example, a nomenclature of CD34⁺, CD31⁻ denotes a cell that expresses CD34 but not CD31. Use of more than one marker can make the cell selection very specific. However, not all cell types have a known specific surface marker [27].

For some cells such as cancer cells, not many cell-surface markers have been identified. In such a situation, some techniques have used a surface marker directed against surface membrane antigens that are expressed in tissue of origin, which is most often epithelial. Thus, detection of these tissue-specific surface markers in the blood stream is suggesting that cancer cells have detached from the tumor. Some techniques attempting to isolate circulating tumor cells (CTCs) from whole blood have used EpCAM, an epithelial cell adhesion molecule that is overexpressed in epithelial carcinomas such as colon and breast. However, published studies have shown inconsistent frequency of EpCAM expression in breast cancer, from as low as 35% to as high as 100% [28-31]. Thus, EpCAM cannot be considered a CTC specific marker. Additional bio-molecules such as DAPI (nucleic acid stain) and antibodies against cytokeratin (expressed on the epithelial cell membrane) and CD45 (expressed on the majority of hematopoietic cells) must be used if captured cells are to be positively identified as CTC. Therefore a cell with the phenotype EpCAM⁺, DAPI⁺, CK⁺, and CD45⁻ is considered a CTC.

The number of available cells of interest poses an additional challenge; in some applications such as the isolation of CTCs from cancer patient or fetal nucleated red blood from maternal circulation, only 1-2 cells are available per milliliter (mL) of whole blood. Specificity is problematic for either method, due to the lack of a cell-specific surface marker/antibody to exclusively detect CTCs or fetal cells [32].

Despite great successes, cell sorting techniques are not ideal and therefore remain an active area of research. In addition to sensitivity and specificity requirements, an ideal technique should not be overly labor intensive, should be automated and quantitative, the results should predict clinical outcome, and help the physician personalize therapeutic options. Automating sample preparation and handling would minimize human errors. Integration of preparation, cell sorting, and post processing will lead to more cost-effective instruments, and alleviate the need for trained personnel and infrastructure. Microfluidic technology enables the precise control over the cell microenvironment during separation, scales down the analyses to very small volume of blood, and has the potential for high-throughput cell separation and analyses.

2. Microfluidic technology

2.1. What microfluidic has to offer?

Microfabrication enables the deposition and etching of thin layers (angstrom to micrometer) of different materials on silicon or glass substrates. These layers can be patterned with accuracy and high resolution, down to the nanometer level using lithography. Lithography is the technique used to transfer a pattern from a mask to the substrate to control the location of the deposition of the next layer or the etching of an existing layer on the substrate.

Microfabricated devices have been used in a broad range of biomedical and biological applications. In the last decade, microchips have been used in microscale sensors for surgical instruments, to monitor physiological activities, in microfluidics applications such as drug discovery and delivery, cell sorting, DNA amplification, electrophoresis, etc. Of relevance to this chapter are the microchips for blood fractionation and cell sorting.

Micromachining consists of a series of robust, well controlled, and well characterized processes that enable the fabrication of microfluidic devices. Such devices can be made cost-effective by the use of any of a wide range of biocompatible polymers or plastics and bulk processing (mass production). The miniaturization of reactions and assays confers many advantages over “macro” scale techniques beyond the obvious reduction in quantities of reagents and materials required per test. The scaling down of volumes results in higher surface to volume ratio: a cube with side length L will scale down by a factor of L^3 , while the surface area will scale down by only a factor of L^2 . Thus, miniaturization results in higher reactivities, shorter diffusion distances, smaller heat capacities, faster heat exchange, shorter assay times, and better overall process control, as well as the capability to integrate multiple steps and to achieve massive parallelization on-chip. Additionally, microfluidic devices are

safer than “macro” platforms due to the smaller chemical quantities used and hence the lower stored energies. A microfluidic device that performs one assay is typically referred to as Lab-on-a-chip, while a device that integrates more than one step is referred to as micro total analysis system (μ TAS) [18].

2.2. Introduction to microfabrication

This section will briefly describe the basic concepts in the microfabrication of microfluidic devices. Microfabrication is the already subject of many textbooks and the interested reader can consult one of these for more in-depth details [33, 34]. Microfabrication is the technology developed by ICs industry to make devices and circuits with feature sizes as small as 14 nm in research, and 45 nm in production. Among these are the microprocessors and the electronic components found in computers, smart phones, television sets, and major other electronic products. Microfabrication is also used for MEMS devices (micro-electro mechanical systems), devices that include a movable part and can be used for sensing. The airbag sensor used to deploy an airbag in a vehicle, the pressure sensors inside car tires, and the electronic compass in a smart phone are all examples of MEMS devices that we unknowingly use every day. BioMEMS, microfluidic devices, and μ TAS are all microfabricated devices similar to MEMS but customized for biological and chemical applications.

Creation of a new microfluidic device includes design of the channel(s), fluid inlet(s) and outlet(s), using a CAD (computer-aided design) software. These softwares, such as CoventorWare® [35], ANSYS CFD [36], COMSOL Multiphysics® [37], can be also used for simulation of the various design parameters such as device dimensions, heat transfer, and flow conditions, therefore narrowing the design space range in which optimum performance should be obtained. The pattern of channels is laid out with the CAD software; this is the 2D design of the device. The depth of the channel will be determined by the etching time. The drawings are transferred to a mask, typically a glass or quartz plate (transparent to UV light), covered with chrome. The chrome is etched (removed) where the UV light will expose the photoresist. The mask, similar to a stencil, transfers the pattern to the photoresist. The device is built on a substrate, which is a silicon, glass or quartz wafer, or a regular glass slide. After substrate cleaning, the photoresist, a photosensitive polymer, is applied. Photoresist is dispensed onto the substrate and it is spun at high speed (2000-4000rpm) to create a thin (1-100 micrometer), uniform and smooth layer. The mask is placed in contact with the substrate and exposed to UV lights on a mask aligner. The photoresist is developed in a developer solution specific for it, and is removed from areas exposed to UV light (positive photoresist). The channels can be etched, with substrate material being removed from areas unprotected by the photoresist. Etching can be either wet (using chemicals) or dry (plasma etching). Deep reactive ion etching (DRIE) is a plasma etching technique typically used to achieve deep channels with vertical side walls. Use of DRIE is necessary if the etched substrate will serve as a template for molding devices in polymer such that the polymer mold can be peeled off the substrate. At this stage, the device can be

sealed by the bonding of a top piece to the substrate. Top pieces are typically transparent, to permit observation under the microscope. Silicon can be bonded to glass by thermal or anodic bonding technique. Usually, however, microfluidic devices are constructed of polymer. Polymers are more cost effective, transparent, and biocompatible materials, many polymer devices can be molded from one silicon master, this is a key advantage because microfluidics devices are hard to clean and hence, can only be used for one or a few experiments.

Polydimethylsiloxane (PDMS), PMMA, polyurethane, and polystyrene are all polymeric materials used for microfluidic devices. PDMS, the most frequently used, comes in the form of two liquid components that are mixed (1:10, w/w) and poured onto the substrate. The PDMS is degassed to remove all air bubbles and ensure that the liquid fills the smallest feature of the mold. PDMS is cured in a 60-80°C oven for 20 to 45 min to solidify. Once solid, it can be peeled off the master substrate. PDMS devices are sealed with glass cover slips to form the channels. Several alternatives to the above described processes exist that can accelerate fabrication. Masks can be printed on transparencies using high-resolution printers; this method is suitable for feature sizes of 100 μm or larger. SU8 is a photoresist that is used to create deep structures for molding eliminating the need for deep etching such as the utilization of DRIE. Utilization of a chrome mask and a well-equipped clean-room facility are necessary for making devices with very small features; sub-micrometer to a few micrometers. The development cycle from concept to prototype can take few weeks. For less fine featured devices, the use of transparencies, polymers, and/or SU8 can be reduce the cost and developmental time to one to few days from concept to prototype [38]. Figure 1a and 1b illustrates the typical processes involved in making channels in silicon and molding devices in PDMS respectively.

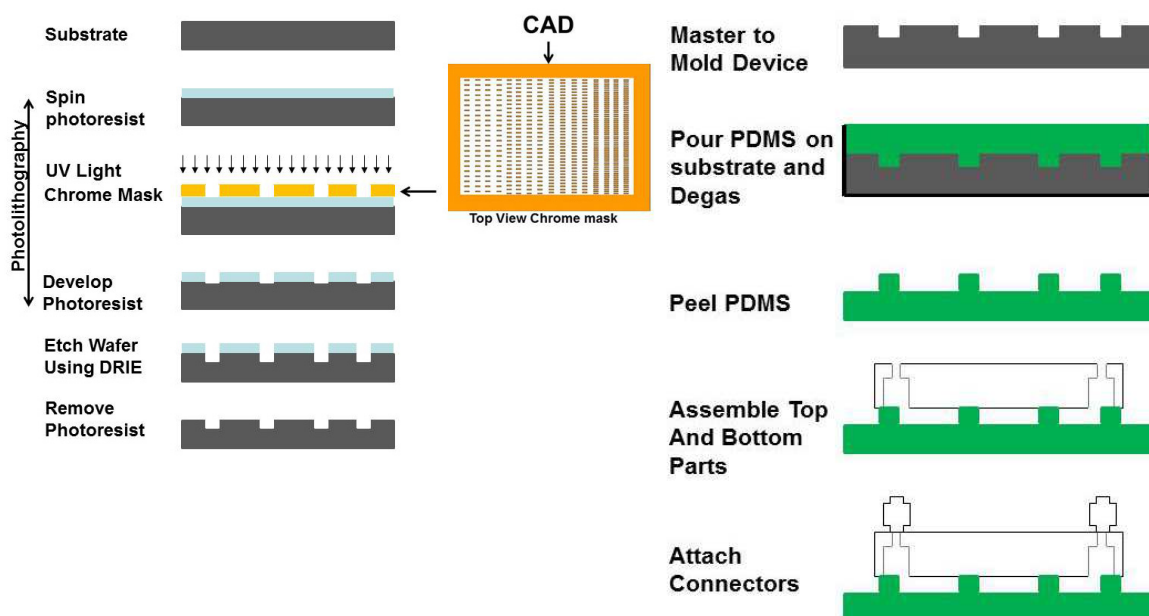


Figure 1. a: Schematic summary of the processes involved in making channel in a hard substrate such as silicon. b: Schematic summary of steps involved in making a PDMS mold from a hard master.

2.3. Types of flow: laminar versus turbulent

Two modes of fluid flow exist: laminar and turbulent. In laminar flow, the fluid moves with slow velocity and each particle of fluid moves in a straight trajectory parallel to the channel walls in the flow direction; and the velocity, pressure, and other flow properties at each point in the fluid remain constant. There are no cross-currents perpendicular to the flow direction, no eddies or swirls of current in laminar flow. Examples are oil flowing slowly through a tube, and blood flowing through a capillary. Turbulent flow in contrast is chaotic, with rapid, spatial and temporal variations of pressure and velocity. Examples of turbulent flow are the blood flow through in arteries, the flow of water through pumps and turbines, and the flow eddying seen in boat wakes and around the wing tips of aircraft [17, 33].

The relative turbulence of a flow can be determined by the dimensionless Reynolds number (Re), which is the ratio of inertial forces to the viscous forces:

$$Re = \rho v \frac{L}{\mu}$$

Where:

ρ is the density of the fluid (kg/m^3),

v is the mean velocity of the object relative to the fluid (SI units m/s),

L is a characteristic linear dimension, (travelled length of the fluid, and

μ is the dynamic viscosity of the fluid ($\text{Pa}\cdot\text{s}$ or $\text{N}\cdot\text{s/m}^2$ or $\text{kg}/(\text{m}\cdot\text{s})$).

Below a certain Re value the flow is laminar; above this threshold the flow becomes turbulent. For macroscopic structures such as pipes with a circular cross-section, the transition from laminar to turbulent flow has been empirically determined at Re of approximately 2300. For most microstructures, in contrast, the Re number is usually low (10^{-1} to 100) thus only laminar flow is relevant for microfluidic devices.

3. Fluid transport process

3.1. Poiseuille flow

A pressure-driven laminar flow inside a tube with a circular cross-section, away from the entrance, is commonly known as *Hagen-Poiseuille* flow or simply *Poiseuille* flow [17, 33]. This flow is governed by the *Navier-Stokes* equations, which are nonlinear, second-order, partial differential equations for describing incompressible fluids. These equations are derived from motion and conservation of mass equations. *Poiseuille* flow is a solution to the *Navier-Stokes* equation, and describes the fluid velocity at any point as a function of the viscosity, pressure, and radius of the tube:

$$V_z = \frac{1}{4\mu} \left(\frac{\partial p}{\partial z} \right) (r^2 - R^2)$$

Where:

V_z is the velocity distribution,

μ is the fluid viscosity,

$(\delta p/\delta z)$ is the z component of the pressure gradient,

R is the distance from the center of the tube, and

R is the radius of the tube.

This equation reveals that the velocity distribution is parabolic, with the maximum velocity occurring at the center of the tube. **Figure 2a**

3.2. Electrokinetic Flow

Electrokinetic flow is the underlying basis of electro-osmosis, electrophoresis, streaming potential, and dielectrophoresis. In electro-osmosis, fluid is made to flow through, by the application of an electric field. The field induces the formation of an electric double layer (EDL). This EDL consists of (1) a compact liquid layer adjacent to the channel surface that has immobile balancing charges, and (2) a second *diffuse* liquid layer, composed of mobile ions. Most solid-liquid, and many liquid-liquid, interfaces have an electrostatic charge, and hence an electric field exists there. In the presence of an electric field, molecules of many dielectric materials, such as the glass or polymer used for making the microfluidic devices, will become permanently polarized, since the material has a dipole that comprises two opposite, but equal, charges, due to the asymmetrical molecular structure. The electrostatic charges on the channel surface, mainly negative charges in the case of glass or polymer, attract counter-ions from the liquid. This attraction creates the channel double layer; the first has immobile charges that balance the charges on the channel surface. The second *diffuse* layer has a higher concentration of counter-ions near the channel surface than does the bulk of the fluid. The net charge density gradually decreases to zero in the bulk liquid. The diffuse layer will move under the electric field. Surrounding molecules are pulled along by a viscous effect, resulting in bulk fluid motion or electro-osmotic flow. The diffuse layer is several nm to 1 or even 2 μm thick, depending on the ionic concentration and electrical properties of the liquid. The *Poisson-Boltzmann* equation describes the ion and potential distribution in the diffuse layer. The electro-osmotic flow velocity can be quantified by Li's equation [39]:

$$V_{av} = E_z \epsilon_r \epsilon_0 \frac{\zeta}{\mu}$$

Where,

V_{av} is the average electro-osmotic flow velocity,

E_z is the applied electric field (V/m),

ϵ_r is the Dielectric constant of the medium,

ϵ_0 is the permittivity of the vacuum,

ζ is the zeta potential at the shear plane, and

μ is the Viscosity.

This equation reveals that the velocity is linearly proportional to the applied electric field, such that all travel at the same speed inside the channel **Figure 2b**. This situation contrasts with the pressure-driven flow, in which the middle has the greatest velocity resulting, in a parabolic migration.

In conclusion, the velocity distribution being parabolic or flat can impact the microfluidic device performance. The electrokinetic flow is favored in applications such as DNA separation, proteomics, rapid mixing, and time dependent applications where sample homogeneity and reaction time need to be stringently controlled. The flow pattern is typically not an issue for cell separation since it happens in continuous flow without time dependence.

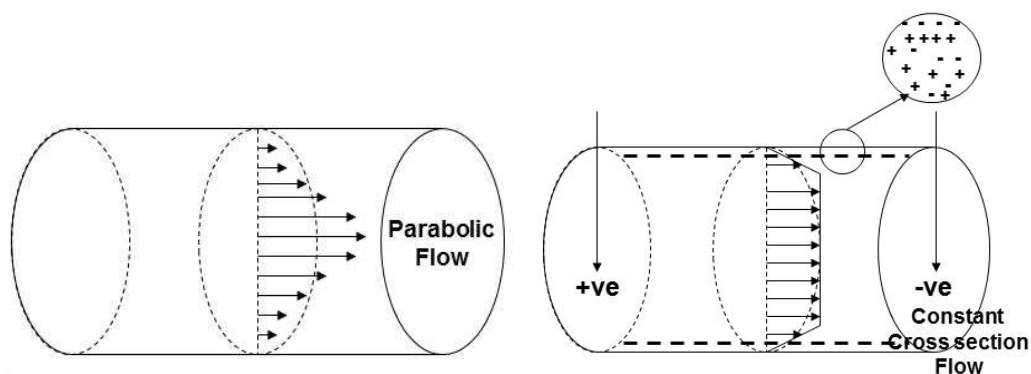


Figure 2. a: schematic of velocity distribution in Poiseuille flow.

b: schematic of velocity distribution in Electro-osmosis flow.

4. Technologies and on-chip mechanisms of separation

Cells are separated either in bulk or individually. In individual cell sorting, each cell is analyzed, and then the cells of choice are individually selected. This technique is rarely used, due to its very low throughput. Thus cells are generally sorted by bulk separation, in which a large number of cells are selected on the basis of shared characteristics such as size, density, or the affinity of a receptor for a specific cell-surface target. The result of such bulk separation is enrichment rather than a true purified population [9].

The cells of interest are first identified, then separated, and finally collected. The initial step is to screen the cells of interest to identify one or more common specific characteristics to be used as the basis of sorting. Specific characteristics can be intrinsic such as size, density, response to electrical or magnetic fields, or resistance to chemical lysis. Alternatively, cells can be labeled using a specific cell surface target that binds to a monoclonal antibody conjugated to a fluorophore, or to magnetic particles for flow cytometric cell sorting.

Once the cells of interest have been identified, they can be separated from the other cell types. In some methods, the identification and separation occur simultaneously, e.g., affinity capture.

In other methods such as fluorescence-activated cell sorting, cells are identified on the basis of the presence or absence of one or more fluorescent tags then are then sorted into two or more separate containers. Sorting can either use negative or positive selection. In positive selection, the target cell itself is labeled; in negative selection, it is the background cells or other cells in the solution that are labeled.

4.1. Separation of cells on the basis of affinity

Affinity chromatography or separation of cells on the basis of their affinity is the fractionation of a cell mixture based on the use of specific immunologic targets. One or more of these specific targets are immobilized on a chip surface; there, they capture the cells of interest with high purity (positive selection), or alternatively they capture large number of background cells so as to enrich the remaining sample (negative selection). Microfluidic devices provide a high surface area to volume ratio, which is necessary for chromatography; to keep processing times manageable, many devices can be used in parallel.

Toner's group demonstrated affinity-based separation of cells based on two specific immunologic targets; CD5 and CD19 [40]. Two microfluidic devices were used for affinity separation: a *Hele-Shaw* device and a parallel flow chamber device. The chamber in the *Hele-Shaw* device was 57 μm deep and 50 mm long, and the inlet was 5 mm wide. The device was fabricated using PDMS and sealed with a glass cover slip. The chip surface was treated with silane solution in ethanol, followed by GMBS in ethanol (a water-soluble amine-to-sulfhydryl crosslinker with a short spacer arm), flushed by Neutravidin (strong affinity to biotin) solution in PBS, and incubated overnight. Antibody, anti-CD5 or anti-CD19, solution stocks were diluted in BSA and sodium azide, flowed through the chamber, incubated for 15 min and then flushed with PBS to remove unattached antibodies. Flow experiments were performed with human immature T-lymphoblasts (MOLT-3 cells) and human mature B-lymphocyte (Raji cells). MOLT3 cells, which express CD5 but not CD19, were stained with green cell-tracker dye. Raji cells, which express CD19 but not CD5, were stained with orange cell-tracker dye. Cells were flowed over the coated chip surface with a syringe pump, at flow rate of 30 or 50 $\mu\text{L}/\text{min}$. Flow rates were optimized for efficient capture to allow dynamic cell adhesion, shear stress was minimized in the axial direction permitting sufficient interaction between the cell and the coated surface so that binding can occur. A device coated with anti-CD19 was used to deplete a 50:50 MOLT-3/Raji cell mixture of Raji cells, producing a 100% pure MOLT-3 in less than 3 minutes. Obviously, this level of enrichment is exceptional and cannot be achieved with a heterogeneous ("real world") blood sample. Nevertheless enrichment by 10- to 2000-fold have been obtained using similar devices [41]. Sin and coworkers also used an alternative parallel flow serpentine chamber design, the effective increase in device length was intended to increase the number of cell capture and also to ensure constant shear stress throughout the device. In summary, Sin and coworkers have demonstrated the possibility of using dynamic cell attachment to antibody-coated microfluidic chambers in shear flow to enrich mixtures of MOLT-3 and Raji cells.

To further increase the chip surface area, Toner's group has developed a microfluidic platform "the 'CTC-chip'" [42]. This device is composed of a two-dimensional array of round pillars.

These pillars are 100 μm in diameter and 100 μm deep; they are separated by 50 μm and each three rows are shifted from the previous three rows by 50 μm to maximize interaction (Figure 3). The chip was etched in silicon with DRIE to produce smooth straight pillars; the result was 78,000 pillars within a surface of 970mm². The pillars were coated with antibody (EpCAM). The chip is enclosed by a manifold. The group had optimized the flow rate allowing adequate cell-pillar interaction time, and to minimize shear forces, ensuring attachment of maximal number of cells to the pillars. The chip successfully identified CTCs in the peripheral blood of patients with metastatic lung, prostate, pancreatic, breast and colon cancer in 115 of 116 (99%), with a range of 5–1,281 CTCs per mL and approximately 50% purity (Figure 3).

Similarly, Chang and coworkers produced two chips with an array of pillars coated with E-selectin IgG chimera, to test the interaction of HL-60 and U-937 cells with these structures [43]. In one device, the square pillars were separated by 25 μm ; each pillar was 25 μm wide by 25 μm long by 40 μm deep. In the second device, pillars were 10 μm wide by 35 μm long by 40 μm deep, and spaced 30 μm apart. In this second device each row of pillars was offset from the previous one by 15 μm so as to allow more cells to be interrogated. Devices were fabricated in silicon by DRIE and were sealed with thin pyrex glass using anodic bonding. In the first device, HL-60 cells were enriched 400 fold over to the original concentration, while the second device achieved only 260-fold enrichment. Offsetting the pillars on the second device had been expected to improve the cell capture, however smaller size resulted in the flow being faster in the channels, thereby increasing shear stress on the cells and making them less likely to be captured on the surface.

It is possible to further increase cell surface interaction if the cells passed through a packed bed of antibody-conjugated beads. However, such a design is no longer attractive since cell crossing takes as long as 2 hr due to the retardation of the flow rate [44].

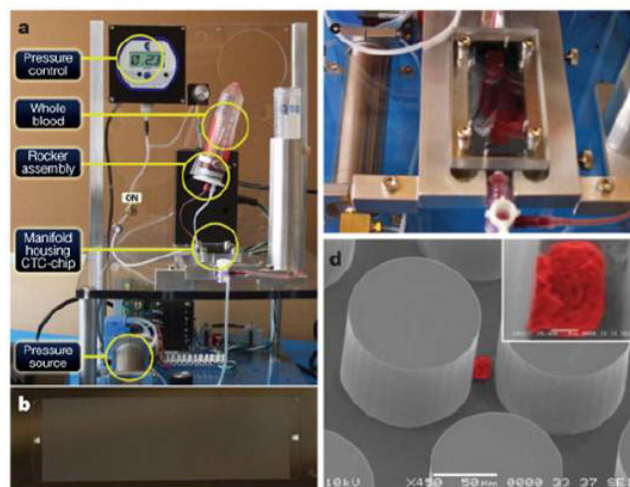


Figure 3. Isolation of CTCs from whole blood using a microfluidic device a, The workstation setup for CTC separation. The sample is continually mixed on a rocker, and pumped through the chip using a pneumatic-pressure-regulated pump. b, The CTC-chip with microposts etched in silicon. c, Whole blood flowing through the microfluidic device. d, Scanning electron microscope image of a captured NCI-H1650 lung cancer cell spiked into blood (pseudo coloured red). The inset shows a high magnification view of the cell (Reprinted with permission from Nature Publishing Group).

Malmstadt and coworkers developed an innovative approach that could benefit from the increased bed of beads area while avoiding its limitation [45]. The group used beads that were modified twice: (i) with the affinity moiety biotin, which binds streptavidin to function as chromatographic affinity separation matrix, (ii) with the temperature-sensitive polymer poly(N-isopropylacrylamide). At room temperature, a suspension of these beads flows through the channel. When the temperature is raised above a certain threshold, the beads aggregate. The sample is then introduced and the beads remain stable during sample flow, and the device functions as a chromatography affinity matrix. The temperature is then lowered below the threshold to allow the beads to dissolve and elute from the channel.

4.2. Separation of cells by flow cytometry

Flow cytometry is a technique that uses light scattering to measure various physicochemical characteristics of suspended cells. Cells are stained and then confined to flow in a single file through a fluidic system. The stream of cells passes at high speed through a focused laser beam. Light scattering and fluorescence data are collected from the individual cells and analyzed. A laser of one wavelength such as blue can be used for excitation; the instrument records fluorescence at multiple wavelengths such as red, orange, and green, in addition to the blue light scattering in the forward direction and right angle to the laser beam. This information is processed by a computer attached to the cell analytical instrumentation. Alternatively, flow cytometers can be equipped to sort cells of interest based on scattering properties, by use of an electric field, flow switching, or optical trapping.

The first key aspect of flow cytometry is the focusing of the cells in a single file so they can be individually interrogated by the optical detection system. This step is usually achieved by hydrodynamic focusing [46, 47]. A sheath flow surrounds the samples from both sides; the flow rate can be adjusted to make the middle stream as thin as required to carry cells in a single file (**Figure 4**). This also reduces cellular aggregation that can clog the device. Microfabricated channel structures are capable of stably delivering samples to a detection area with higher accuracy and better flow control than are glass capillary-based fluidic systems used in conventional flow cytometric equipment; this superior performance is a function of the small channel dimensions possible in microfluidics. The hydrodynamic focusing typically constrains the cells on both sides, but not in the z direction [48].

Miyake and coworkers have developed a multilayered sheath flow chamber that can generate a three-dimensionally focused narrow stream. The channel system was formed by the lamination of five separate silicon and glass plates; defining the three-dimensional geometry of a sample injection nozzle and a detection microchannel. A simpler, albeit less flexible or programmable, approach would be to use a shallow channel that confined the cells in the z direction to remain within the analysis window [49].

Sheath liquid-based hydrodynamic focusing, while being the standard technology in microfabricated flow cytometers, require continuous pumping of a large volume of sheath liquid at a high flow rate to pinch the middle stream down to single-cell width. Sheath

liquid volume required can be up to 1000 times the sample volume. New types of microfluidic systems have been developed to minimize or eliminate the sheath liquid requirements and to further miniaturize flow cytometry. Huh and coworkers demonstrated the use of ambient air as an alternative sheath fluid in a disposable air-liquid two-phase microfluidic system [50]. The system produces a thin ($>100\ \mu\text{m}$) liquid stream transporting cells focused by air-sheath flows in a rectangular microfluidic channel. To achieve this focusing, the authors had to conduct a detailed study of the PDMS surface wettability, and of the flow conditions so as to overcome the two-phase (air-liquid) instabilities.

In a contrasting approach, a V-shaped groove device was developed by Altendorf and coworkers to transport blood cells in a single file. The groove microchannel was fabricated by anisotropic wet etching of silicon [51]. The top of the groove was 20–25 μm wide and the constriction channel geometry allowed the generation of a single-file stream of blood cells moving through the channel without the need for sheath fluid. Light scattering caused by the flow of the individual blood cell through the device was measured by optics based on a photomultiplier tube, photodiode detector, and laser source. The device was capable of differentiating between various cell populations such as RBCs, platelets, lymphocytes, monocytes and granulocytes, based on the intensity of scattering signals. This study demonstrated the potential utility of such a device for differential counting of blood cells.

The second aspect of a flow sorter system that is pertinent to our discussion is the system capability to sort cells at high speed. The requirement of rapid deflection after the cell has been identified by the optical system, can be achieved through redirection of the flow via high-speed valving or reverse electrokinetic flow, dielectrophoresis, ultrasonic transducer, or optical trapping.

Kruger and coworkers achieved switching by use of pressure-driven flow systems [46]. As a liquid sample stream that was hydrodynamically focused along the center of an input channel approaches a junction, a small amount of buffer liquid is injected into or withdrawn from the side stream along a switch channel, causing the focused sample stream to be deflected and to flow into a collection channel.

Fu and coworkers demonstrated the use of electric field to quickly switch the flow from the waste to the collection channel, to isolate a cell of interest [52]. The disposable activated cell sorter consisted of three channels joined at a T shaped junction. Electro-osmotic flow drives cells or particles from the inlet to the junction where the flow is diverted to the waste or collection channels. The diversion is achieved by a switching of the electric field at the T junction to control the flow in a rapid manner. This device does not use sheath flow but rather a small-diameter channel, to constrain the cells in single file. When the fluorescently tagged bacterial cell of interest is detected, the sample stream flowing from an inlet to a waste port is quickly switched by reversed electric field, such that the flow is diverted direction to a collection port, selectively delivering the labeled target particles to a sample collector. Using this fluidic switching-based sorting technique, the authors demonstrated sorting of fluorescent microbeads and *E. coli* cells at a throughput of ~ 10 beads s^{-1} and ~ 20 cells s^{-1} . The device was fabricated by softlithography in PDMS.

Similarly, Oakey and coworkers demonstrated the use of electric field for diverting the flow rather than switching since their device did not have hydrodynamic focusing [53].

Johansson and coworkers developed an ultrasound transducer that was placed in the middle of the channels at the intersection between the waste and collection channels. In the absence of ultrasound wave, cells migrated to the waste channel. When a cell of interest was identified, the transducer produced a radiation force acting on a density interface that caused fluidic movement, and the particles or cells on either side of the fluid interface were displaced in a direction perpendicular to the standing wave direction toward the collection channel [54].

Chun and coworkers demonstrated a polyelectrolytic salt bridge-based electrode, placed across the channel to replace the laser used for cell fluorescence analyses. The salt bridge produced impedance signals in proportional to cell's size to be used as basis for sorting to eliminate the need for the optical system that typically exist off-chip [55].

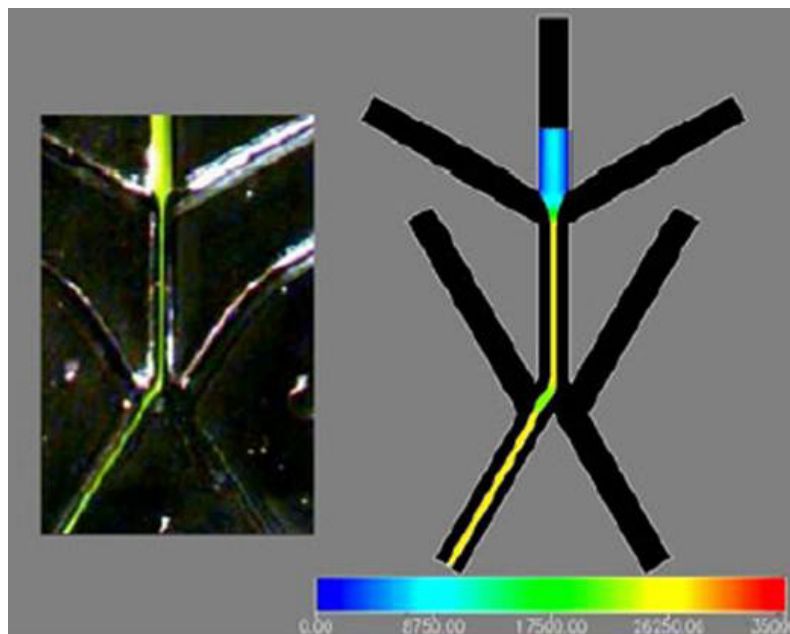


Figure 4. Left: Image of prototype device in operation. Right: Computational modelling of fluid dynamics in a microfluidic cell sorter structure. The performance of this structure was simulated using FlumeCAD (Microcosm Technologies), a finite element modelling (FEM) software package that uses full Navier–Stokes equations. (Printed with permission from Institute of Physics Publishing).

4.3. Separation of cells using immunologic targets

Magnetic separation can be achieved by using the cell's intrinsic magnetic properties or by attachment of a magnetic particle to a specific surface antigen that can later be exposed to a magnetic column for separation. Magnetic particles are typically composed of large numbers of superparamagnetic nanoparticles packed inside micrometer sized sphere made of polymer. The surface of each magnetic bead is then functionalized with antibody specific to an antigen found on the surface of one type of cell. The cells are incubated with the

magnetic beads to allow interaction; the magnetic bead attaches specifically to the cell by the antibody-antigen recognition. The cells are transferred to the magnetic column of a separation device. The cells are then manipulated via a magnetic field generated by an internal patterned electromagnet or external macroscopic magnets. The cells attached to the magnetic beads stay on the column, while other cells, not expressing the antigen, and hence not attached to beads, flow through it. With this method, the cells can be separated positively or negatively with respect to the particular antigen(s). Positive selection results in the binding of the cells of interest to the column and they then need to be washed off of the column. In negative selection, the cell of interest do not bind, and are passed through the column enriched [56].

Han and coworkers have exploited the intrinsic differences in the magnetic properties of the RBCs and WBCs without use of magnetic beads, to separate the cell types in a one-stage or three-stage magnetophoretic microseparator [57]. Their single-stage device was able to separate 91% of RBCs out of whole blood; the three-stage device improved on this performance to separate 93.5% of RBCs and 97.4% of WBCs from the whole sample at 5 $\mu\text{L/hr}$ flow rate. Qu and coworkers demonstrated identical separation efficiency [58]. Han's channels were 50 μm deep created by hydrofluoric acid etching of borofloat glass slides. The wire area, included to deform the magnetic field inside the channel and hence generated a high field gradient, was defined using photolithography, and a Ti/Cu/Cr seed layer was deposited by e-beam evaporation, followed by microelectroforming (a process for making thick metal structure) of the ferromagnetic nickel wire. The device was sealed with a second glass slide by thermal bonding. An external magnet provided the magnetic field.

Adams and coworkers developed a multi-target magnetic cell sorter to purify two types of target cells. They simultaneously sorted (i) multiple magnetic tags achieving >90% purity and >5,000-fold enrichment, and (ii) multiple bacterial cell types achieving >90% purity and >500-fold enrichment, with a throughput of 10^9 cells per hour [59]. Their device incorporates microfabricated ferromagnetic strips (MFS) to generate large and reproducible magnetic field gradients within its microchannel and utilizes a multistream laminar flow architecture to accurately control the hydrodynamic forces. This design enables continuous sorting to of multiple target cells into independent spatially addressable outlets with high purity and throughput.

The chip was fabricated in three layers: glass-PDMS-glass. The channel was 50 μm deep and 500 μm wide, and contained two sets of 20-200 nm thick nickel patterns that compose the MFS structures. (Figure 5) The two sets of MFS arrays are aligned at different angles with respect to the flow direction. The result is that two magnetophoretic forces that differ in amplitude and direction, act on the labeled cells. The labels are different in size and magnetization and thus require different forces to deflect them out of the stream of laminar flow. The magnetic field is created with a magnet made of a custom stack of neodymium-iron-boron (NeFeB) and placed underneath the chip. The MT-MACS sorting chip was used to sort two subtypes of *Escherichia coli* MC1061 cells. One type was labeled with label 1 with

tag 1 ($r = 2.25 \mu\text{m}$, $M = 14 \text{ kA/m}$) and tag 2 ($r = 1.4 \mu\text{m}$, $M = 30 \text{ kA/m}$), and was fluorescently labeled for observation under a fluorescent microscope. Using 5 mL/hr flow rate, each of the tags was enriched several thousand fold at its respective outlet after a single round of purification. At outlet 1, the population with tag 1 was enriched from 0.020% to 95.876% of the total population corresponding to a $5,000$ -fold enrichment. The impurities in this fraction consisted of 2.974% tag 2 and 1.150% nontarget beads. Similarly, the population with tag 2 in outlet 2 was enriched $15,000$ -fold, with contamination of 3.125% target 1 and 6.358% nontarget beads. The waste output consisted almost entirely of nontarget beads (99.997%), and contamination of 0.002% of tag 1 and 0.001% of tag 2.

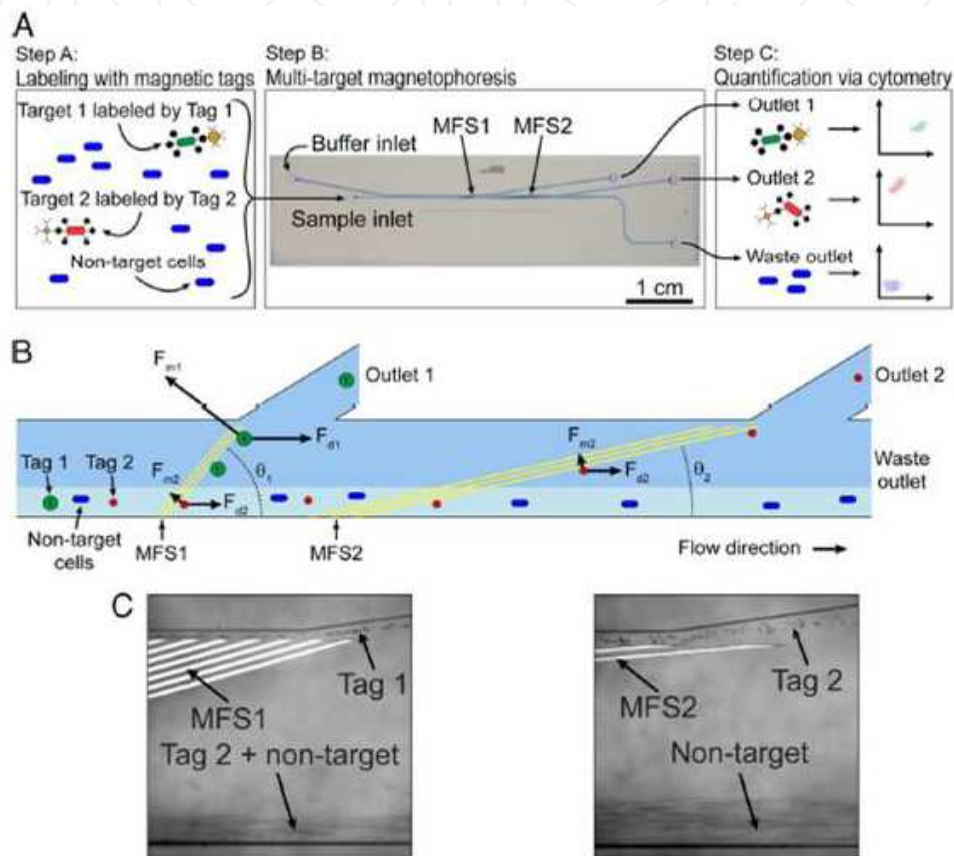


Figure 5. MT-MACS separation architecture. (A) (Step A) The sample contains an excess of nontarget cells and 2 different target cells (target 1 and target 2) that are labeled with 2 different magnetic tags (tag 1 and tag 2) by specific surface markers. (Step B) The sample is continuously pumped into the device where the 2 target cell types are sorted into spatially-segregated independent outlets. Separation occurs in 2 regions of high magnetic field gradient generated by the microfabricated ferromagnetic strip (MFS) 1 and MFS 2. (Step C) After sorting, the eluted fractions from each outlet are analyzed via flow cytometry. (B) A free-body diagram showing the balance of forces at the MFS structures. At MFS 1 ($\theta_1 = 15^\circ$), tag 1-labeled target 1 cells are deflected and elute through outlet 1 because $F_{m1} > F_{d1} \sin(\theta_1)$. This is not the case for tag 2-labeled target 2 cells, which are instead deflected at MFS 2 ($\theta_2 = 5^\circ$) because $F_{m2} > F_{d2} \sin(\theta_2)$, and elute through outlet 2. Nontarget cells are not deflected by either MFS and elute through the waste outlet. (C) Optical micrographs (magnification $\times 100$) of the tags being separated at the 2 MFS structures at a total flow rate of 47 mL/h (sample $\approx 5 \text{ mL/h}$, buffer $\approx 42 \text{ mL/h}$). (Left) Tag 1 is deflected by the steep angled MFS 1. (Right) Tag 2 is deflected by MFS 2 (Reprinted with permission from PNAS).

Xia, Modak and coworkers used similar have demonstrated similar magnetic cells sorting design with the structure concentrating the magnetic field being adjacent to the flow channel but not exposed to the sample solution [60, 61].

Lee and coworkers demonstrated the use of patterned channels to magnetically manipulate single cell. Lee's device had a matrix of two separate layers of straight gold wires, each addressed independently, aligned perpendicular to each other, and covered with an insulating layer. A magnetic field was created by passing electrical current through the wires creating a programmable magnetic field to control the motion of individual cells in the fluid. Lee's device demonstrated the separation of viable from nonviable yeast cells attached to magnetic beads [62].

Saliba and coworkers demonstrated a 2D array of dots by deposited by microcontact printing of a magnetic ink acting as magnetic traps. Antibody-coated magnetic beads were injected in the channels and were submitted to a Brownian motion in the absence of any field. The application of an external vertical magnetic field induced the antibody-coated magnetic beads to assemble on the patterned dots creating columns [63].

Kose and coworkers demonstrated a novel device to use colloidal suspension of nonfunctionalized magnetic nanoparticles for manipulation and separation of microparticles. It is a size-based separation mediated by angular momentum transfer from magnetically excited ferrofluid particles to microparticles. The nanocytometer is capable of rapidly sorting and focusing two or more species, with up to 99% separation efficiency [64].

4.4. Separation of cells using chemotaxis phenomena

Chemotaxis is the process whereby a single cell, or multicellular organism, moves away or toward a certain chemical. This movement can be away from a poison (chemorepellent or negative chemotaxis) or toward food (chemoattractant or positive chemotaxis). For example, neutrophils leave the blood vessel and migrate toward the smell produced by bacteria in a cut of the skin in an effort to defend the body against infection. The influence of these gradients of molecules and cues cellular behavior in the surrounding microenvironment is an important biomedical focus of study. Chemotaxis, in particular, plays an important role in many biological and physiological processes such as creation of new tissues, wound healing, cancer metastasis, and embryogenesis.

To test a cell response to a certain chemical gradient, the cells are typically placed in a well, and the test substance or chemical is placed in a second well. The two wells are separated by a barrier such as a weir structure (Dunn chamber) or a filter (Boyden chamber), to ensure that the cell movement is due only to the signaling only and not random motion or diffusion.

The development of microfluidic devices for chemotaxis assays was motivated by the need to produce the gradient in a controllable and reproducible manner, and to minimize the quantities of test substance and cells required per assay [65].

Abboodi and coworkers have developed a hydrogel-based microfluidic chip for chemotaxis studies [66]. The device consists of three chambers in this study, the middle chamber is filled with a 3D porous hydrogel structure that contains the cell culture; here fibrosarcoma cell line HT1080 was used as an invasive cancer cell model. First, the left-hand chamber was filled with a cellulose enzyme solution and the right-hand one was filled with cell culture medium containing fetal bovine serum (FBS) (Figure 6). The cellulose enzyme solution diffuses into the hydrogel and degrades it, creating large pores in the structure closer to the left-hand reservoir. Pore size is progressively smaller as the solution migrates toward the right-hand reservoir. The result is that the cells, stained for observation by fluorescence microscopy, moved toward the large pores adjacent to the left-hand reservoir. After 3 days, the FBS –containing medium-FBS in the right-hand reservoir was replaced with pure FBS i.e., full strength chemoattractant. The cellulose enzyme solution in the left-hand reservoir was also replaced with a FBS-containing medium. In response, the cells reversed their motion and moved toward the right-hand reservoir containing the pure FBS, confirming that FBS is a chemoattractant for this cell type. The negative structure of the chambers of this device was fabricated with a 3D printer and a UV-curable polymer. The device was molded in PDMS from the polymer structure and sealed with a glass slide.

Agrawal and coworkers, in an effort to explore the sepsis complications that occur in burn patients, presumably as the result of improper activation of neutrophils, developed an assay on an advanced switching gradient device for monitoring the migration behavior of these cells following thermal injuries [67]. The device (i) integrates the isolation of neutrophils from whole blood, (ii) the provision of a controlled combinatorial chemotactic environment, and (iii) the monitoring of real-time migration of the captured neutrophils over different substrates all on-chip, thereby eliminating the need for preprocessing of the blood. The device was made with PDMS and was fabricated with standardized soft lithographic techniques. In a first trial, the capture was performed by a coating of the microfluidic cell chambers with P-selectin, E-selectin, or fibronectin substrate. A 10 μL drop of blood/heparin solution was loaded in the cell-capture device, and the cells were allowed to settle for 10 min; then flow was initiated (0.5 $\mu\text{L}/\text{min}$) and most of the unwanted cell population was washed away. In experiments repeated in the migration device, captured cells were exposed to a linear chemotactic gradient of the chemokines IL8 and fMLP. Migration patterns for both chemokines over each substrate were recorded with time lapse microscopy and were then compared.

The two chemoattractants, IL8 and FMLP, were used to create a gradient across each binding substrate. Neutrophils over P-selectin reacted similarly for the IL8 and fMLP gradients. However, for E-selectin, average 'y' displacements of 50 μm and 70 μm were observed within 30 min in the gradients of fMLP and IL8 respectively.

For fibronectin, the difference in migration was more significant: the cells migrated about 65 μm in fMLP gradient, but only 35 μm in the IL8 gradient over similar time courses. This system offers an efficient approach to the development of a simple diagnostic tool suitable

for a variety of applications in addition to chemotactic studies such as genomic and proteomic analyses.

Chen and coworkers demonstrated a cell migration chip which can monitor chemotaxis at single cell resolution [68]. The chip is composed of weirs that captured individual cells. Once a cell is captured, the hydrodynamic force will push other cells to the next weir through a serpentine channel. A high capture rate over 94% is achieved by optimizing the geometry of capture sites and the length of serpentine structures. After capturing, cell migration experiments induced by chemotaxis were carried out using the fabricated platform, and the behavior of each single cell was successfully traced.

Englert, Walker, and coworkers focused their effort on generating reproducible gradients [69, 70]. Engelrt and coworkers device created reproducible chemoeffector gradients. Two gradients, to simulate competing conditions in nature, were created using a Laminar flow-based diffusive mixing and were tested on *Escherichia coli*. The sample containing the fluorescently stained *Escherichia coli*, for observation by microscopy, was introduced in a middle channel. Two side channels introduced the two gradients: quorum-sensing molecule autoinducer-2 (AI-2) and stationary-phase signal indole were introduced, one on each side of the sample. Results showed that the *Escherichia coli* was attracted by the AI-2 and repelled by the stationary-phase signal indole.

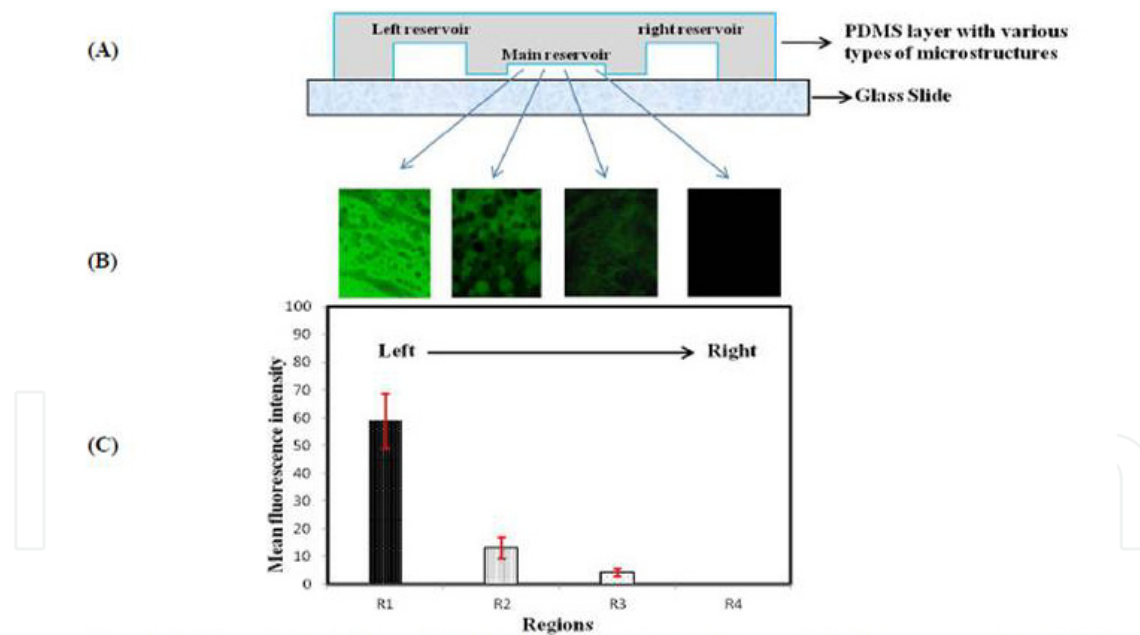


Figure 6. (A) Schematic for the device. (B) Image for each region in the main storage. (C) Average fluorescent intensity of FITC- BSA at four regions from left to right through the porous hydrogel in the main storage \pm SD (Reprinted with permission from SPIE and A. Al Abboodi).

4.5. Separation of cells using optical methods and light trapping

Optofluidics technology, which is the mating of optical trapping, switching, and microfluidic has been recently introduced as a new manipulation scheme. It has been

motivated by its high selectivity, ability to maintain sterility, and how it allowed programmable manipulation of particles or fluids in microenvironments based on optically induced electrokinetics. While optical switching is often used with flow cytometry as the switching or sorting mechanism, it is here presented in a separate section to demonstrate its unique capabilities and potential. Typically, a focused laser beam provides a force to hold or move a microscopic dielectric particle. The dielectric particle is attracted to the strong electric field gradient at the narrowest point of the focused beam. This force is small, in the order of piconewtons, depending on the refractive index mismatch, and can be attractive or repulsive.

MacDonald and coworkers introduced a bow-tie like chip with four reservoirs linked in the middle by a flow channel (Figure 7). The two reservoirs on one side are for buffer (top) and sample (bottom) respectively. The two reservoirs on the other side are for waste (top) and sample collection (bottom). In the absence of any force, the cells migrated from their reservoir to waste, while the buffer passed to the collection reservoir. The two flows shared the channel but no mixing due to laminar conditions. When optical forces were focused on the flow of mixed particles as it passed through the lattice, selected particles were strongly deflected from their original trajectories into the collection reservoir, while others passed straight through, depending upon their sensitivity to the optical potential. The interaction with optical fields provided a selective means of removing material matching specific criteria from an otherwise laminar stream. The optical force was applied by the mean of a five-beam interference pattern created by a 1,070-nm laser beam that passed through a diffractive beam splitter, producing four beams diverging from the central, non-diffracted, in a cross shape. Collimating optics provided a parameter space to independently control the phase and amplitude of each of the five beams before being co-focused through an aspheric lens to produce a large, three-dimensional optical lattice through multibeam interference [71].

Kovac and coworkers introduced a microwell array that is passively loaded with mammalian cells via sedimentation. These cells were inspected using microscopy. After inspection, cells of interest were levitated from the well using a focused infrared laser into a passing stream to the collection reservoir. This is a simple device made of PDMS for the channels and the wells were sealed with glass slide [72].

Shirasaki and coworkers used optics to control a thermoreversible gelation polymer (TGP) as a switching valve. The chip has Y-shaped microchannels with one inlet and two outlets. The sample containing fluorescently labeled cells was mixed with a solution containing the thermoreversible sol-gel polymer. The fluorescently labeled target cells were introduced in the channels and observed using fluorescence microscopy. In the absence of a fluorescence signal, the collection channel was plugged through laser irradiation of the TGP and the specimens were directed to the waste channel. Upon detection of a fluorescence signal from the target cells, the laser beam was then used to plug the waste channel, allowing the fluorescent cells to be channeled into the collection reservoir. The response time of the sol-gel transformation was 3 ms, and a flow switching time of 120 ms was achieved. The TGP did not affect cell viability [73].

Lin and coworkers have demonstrated a microfluidic system based on a computer controlled digital image processing (DIP) technique and optical tweezers for automatic cell recognition and sorting in a continuous flow environment. In this system, the cells are focused electrokinetically into a narrow sample stream and are introduced into the channel where they are recognized and traced in real time. Synchronized control signals generated by the DIP system are then used to actuate a focused IR laser beam to displace the target cells from the main sample stream into a neighboring sheath flow, which carries them to a downstream collection [74].

In summary, Optoelectrofluidic technology, which has been recently introduced as a new manipulation scheme, allows programmable manipulation of particles or fluids in microenvironments based on optically induced electrokinetics. The behavior of particles or fluids can be controlled by inducing or perturbing electric fields on demand in an optical manner, which includes photochemical, photoconductive, and photothermal effects [75, 76].

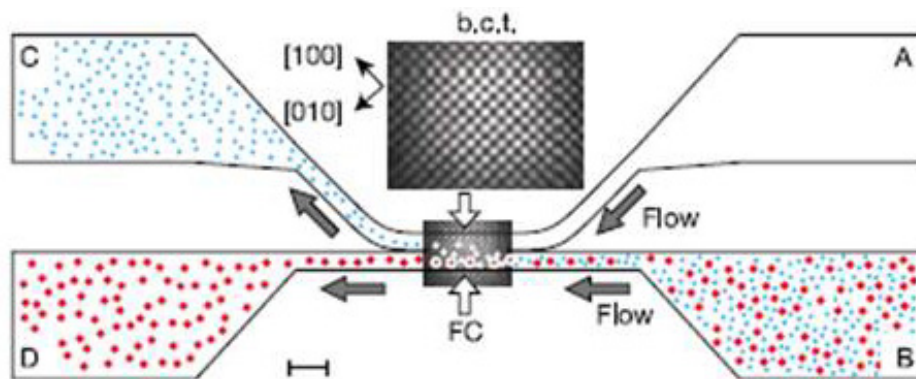


Figure 7. The concept of optical fractionation. Low Reynolds number flows will be laminar: without an actuator all particles from chamber B would flow into chamber D. Chamber A would typically introduce a 'blank' flow stream, although this could be any stream into which the selected particles are to be introduced. By introducing a three-dimensional optical lattice—in this case a body-centred tetragonal (b.c.t.) lattice—into the fractionation chamber (FC), one species of particle is selectively pushed into the upper flow field. The reconfigurability of the optical lattice allows for dynamic updating of selection criteria. For weakly segregated species, the analyte can be either recirculated through the optical lattice or directed through cascaded separation chambers. This latter option also allows the use of multiple selection criteria in a single integrated chip. The flow volume in our current sample cells is 100 μm thick; scale bar, 40 μm (Reprinted with permission from Nature Publishing Group).

4.6. Separation of cells using electrophoresis and dielectrophoresis

Dielectrophoresis (DEP), first described by Pohl in 1951, is a phenomenon in which a force is exerted on a dielectric (insulator that can be polarized) particle when subjected to a non-uniform electric field. This can take place in either direct (DC) or alternating (AC) electric fields. The strength of the force depends on the frequency of the electric field, the medium and particle electrical properties, and the particles size and shape. Varying the field's frequency can manipulate particles with different sizes with great selectivity, which is used for manipulating cells and nanoparticles.

Pommer and coworkers have used DEP phenomenon to separate platelets directly from diluted whole blood in microfluidic channels. Since platelets are the smallest cell type in blood, DEP-activated cell sorter (DACS) was used to perform size based fractionation of blood samples and continuously enrich the platelets [77].

Hu and coworkers used a comparable device to Pommer, but the difference in size-based separation was attributed to the size of the antibody-conjugated beads attached to the target instead of the cell's intrinsic size [78]. Pommer's device is composed of two identical purification stages, in each stage a buffer is introduced in the middle of the channel while the sample is loaded from both sides. The channel electrodes are at angle with the flow forming a funnel shape where the sample flows from the wide to the narrow side. The force exerted by the electric field on the cells has a cubic dependence on the radius ($\propto R^3$) and can be controlled by varying the applied voltage. The hydrodynamic drag force under laminar flow has a linear dependence on the particle radius ($\propto R^1$) and is controlled by varying the flow rate. Therefore, the resulting forces exerted on the cells has a square dependence ($\propto R^2$) and is used to deflect large cells (RBCs and WBCs) into the middle buffer stream to the waste collection reservoir while the platelets remain in the side flow and migrate to the collection reservoir. Post sorting cytometric analysis revealed that a single pass through the two-stage device yields 95% purity of platelets with minimal platelet activation. Two Borosilicate glass wafers were used to fabricate the top and the bottom of the device, the titanium-gold (20nm and 200nm respectively) electrodes were patterned and evaporated using e-beam, a polyimide layer was spun and patterned to form 20 μ m channel depth between the top and bottom wafer. The two wafers were aligned and bonded using thermal bonding (300°C) then 375°C to cure the polyimide.

Vahey et al have extended DEP to multiple electrodes creating an electric conductivity gradient to separate cells and particles. This is similar to using isoelectric focusing in analytical chemistry and proteomics with the conductivity replacing the pH gradient. Vahey et al have used this device to achieve label-free separation of multiple (>2) subpopulations from a heterogeneous background. The channel was 1mm wide and 20 μ m deep molded in PDMS and sealed with pyrex wafer that has the evaporated electrodes. The six electrodes, 200nm gold on top of 10nm titanium (adhesion layer) are 60 μ m wide, separated by 15 μ m, and are patterned at an angle with the flow direction. The electrical gradient was used to separate 1.6, 1.75, and 1.9 μ m polystyrene beads from a mixture. Additionally the device was successfully used to separate similar size beads based on surface conductance due to different coating such as COOH modified and unmodified, as well as sorting nonviable from viable cells of the budding yeast *Saccharomyces cerevisiae* [79].

Lapizco-Encinas et al have used insulator-based (electrodeless) dielectrophoresis (iDEP), in which the nonuniform electric field needed to drive DEP is produced by insulators, avoiding problems associated with the use of electrodes [80]. This channel was 10.2mm long and contained a two dimensional array of 10 μ m deep pillars etched in borosilicate glass. The channel was thermally bonded with a drilled cover plate for fluid access. Two platinum wires, the only electrodes in the device, were placed in the inlet and outlet reservoirs,

producing mean electric fields of up to 200 V/mm across the insulators. The insulator posts disturbed the electric field lines, squeezing them between the pillars. This created higher field strength between the pillars. Cell trapping and release were controlled by modifying the relative responses of electrokinetics and DEP by adjusting the magnitude of the applied voltage. Dead cells had significantly lower dielectrophoretic mobility than live cells but similar electrokinetic mobilities. Therefore, live cells were concentrated between the pillars. Cells were labeled with Syto 9 and propidium iodide for observation through a fluorescent microscope (Figure 8).

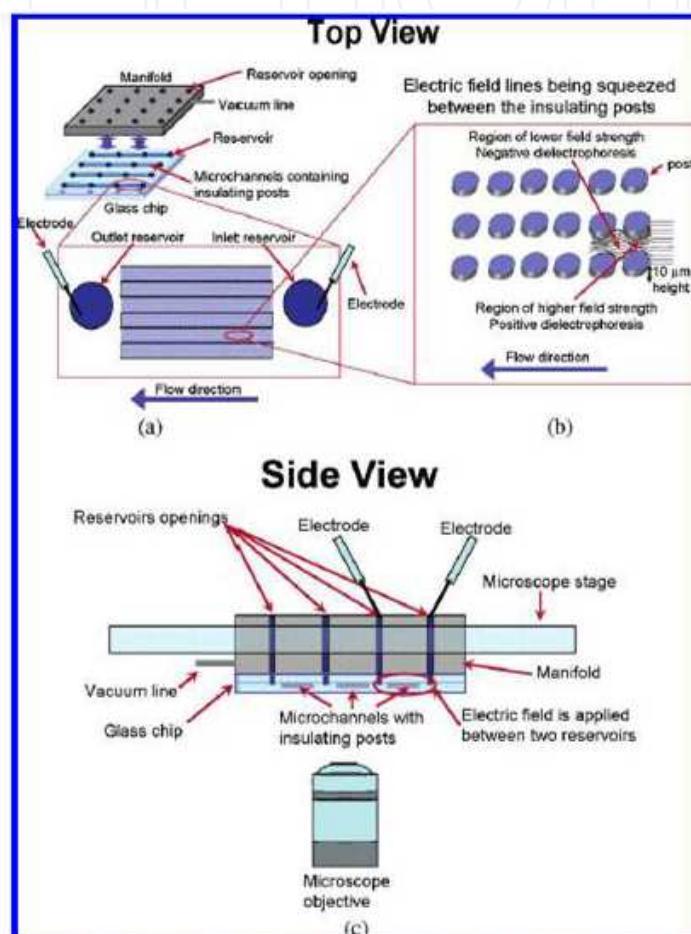


Figure 8. Schematic representation of the experimental setup: (a) top view, showing the manifold, glass chip, an enlargement of the flow microchannels; (b) cartoon showing the electric field lines being squeezed between the insulating posts; (c) side view showing the manifold and glass chip on the microscope stage (Reprinted with permission from ACS Publications).

4.7. Separation of cells by size

Size-based sorting has been our work's focus for a few years; we have successfully demonstrated the separation of WBCs, RBCs, or circulating tumor cells from whole blood, and fetal nucleated red blood cells (fNRBCs) from cord blood. Size- and density-based sorting has been demonstrated in open flow channels by Seki's group using "pinched flow fractionation" [81]. Enrichments up to 20 fold have been accomplished by the chip shown in

Figure 9. The sample is loaded into the 20 μm wide open channel, and a second solution, a buffer, is loaded from a second channel that is 200 μm wide. The buffer pinches the flow width against the channel wall down to 15 μm , forcing the cells to align along the channel wall, before the channel opens to a 350 μm wide area with 12 outlet ports. The separation occurs in the wider channel; the smaller, lower-density cells segregate and are dragged along the channel wall, while the larger, denser cells, tended to sediment earlier in the pinched region and occupy the outer stream that empties to a different outlet port. The device was fabricated by standard photolithographic techniques and was molded in PDMS, from an SU8 master. Wilding's group used weir-like structure to create a 3.5 μm space between the silicon bottom and a glass top of a device to separate WBCs from whole blood, they could then use the cell's DNA for amplification [82-84].

Austin's group has demonstrated cell sorting based on asymmetric bifurcation of a laminar flow around a periodic array of micrometer-scale pillars [85, 86]. Each row of pillars is offset horizontally with respect to the previous row by a fraction of the distance separating the pillars. This offset between successive rows forces particles to navigate around the obstacles and induces a lateral displacement proportional to their size. Therefore, cells or particles of different sizes exit the array at different locations and can be collected separately. The main advantage of such a device is that it never clogs, since the distance between the pillars is always larger than the cells or particles they separate. This device was used to fractionate a mixture of different-diameter beads; 0.8, 0.9, and 1.03 μm into three distinct streams. Additionally, this device was used to separate a mixture of DNA molecules, 61 and 158 kb, in two separate trajectories. In this case an electric field of 12V/cm was used to drive the flow.

Additionally, Austin group has used a variation of this chip to separate RBCs, WBCs, and platelets from blood plasma [87].

Our group has employed pillar configuration to create multiple sieving devices for size-based separation. With these devices, we have demonstrated the isolation of cultured cancer cells spiked into whole blood [88]. Our devices have successively narrower gap widths between the columns in the direction of flows with 20, 15, 10, and 5 μm spacings all on one device (**Figure 10**). The first 20 μm wide segment disperses the cell suspension and creates an evenly distributed flow over the rest of the device, whereas the other segments were designed to retain successively smaller cells [89]. The channel depth is constant across the device. Two types of devices were constructed, the first type was 10 μm deep and the second type was 20 μm deep. As cells traversed the device, they continued through each region until they were stopped at a gap width that prohibited passage due to their size. Experiments with human whole blood, from healthy individual, proved that channels 5 μm wide and 10 μm deep permitted all normal cell types to cross without resistance under our experimental flow conditions. Cultured cancer cell lines, mixed with whole blood and applied to the device, were retained inside the device while all other cells migrated to the output reservoir.

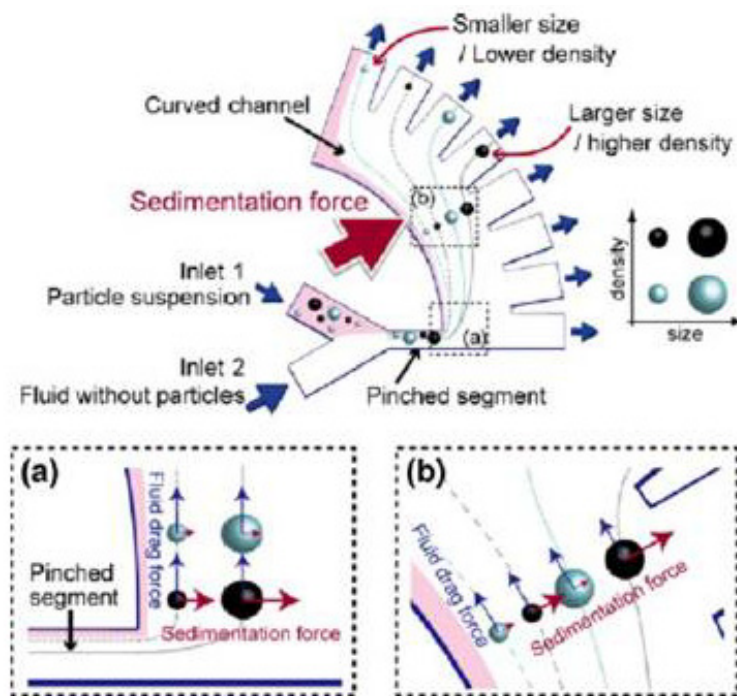


Figure 9. Schematic illustrations showing the separation mechanism of sedimentation pinched-flow fractionation. Images a and b show enlarged views of areas (a) and (b) of the upper image, respectively. In the pinched segment, particles are focused onto the upper sidewall regardless of size. By applying sedimentation force to the flowing particles in the curved channel, particles with a higher density (black) migrate beyond the streamline, achieving density-based sorting. (Reprinted with permission from Springer publisher.)

Eight different cancer cell line, brain neuroblasts (SK-N-MC, SK-N-AS, SK-N-SH, BE(2)-M(17), and SH-SY5Y), breast epithelial cells (MDA231), colon epithelial cells (SW620), and kidney epithelial cells (HEK293), were successfully isolated from whole blood by our device. Additionally, either intact cells, or DNA, could be extracted for molecular analysis. DNA was extracted by *in-situ* cell lysis. After the cancer cells had been retained, the device was flushed for 20 min, with medium used to remove all non-retained cells, followed by water to lyse the retained cells and release their DNA. DNA was collected from the output reservoir for 20 min (approximately 0.33 mL), purified, and tested, as a demonstration that the captured DNA was from the cancer cell line and not a contaminant DNA from the blood used for spiking.

Alternatively, retained intact cells were recovered by reversing the direction of the flow, using medium after allowing 20 min for them to migrate towards the outlet. Once flow was reversed, cells retained at the first row of transition at the 10 μm wide channels detached easily and traveled through the 15 μm and then the 20 μm segments, through the inlet reservoir, and into a collection tube. Cells were cultured from the collection tube and were able to proliferate, thus demonstrating the viability of the extracted cells.

Our device was made using standard photolithography techniques and was molded in PDMS, polystyrene, or polyurethane [90].

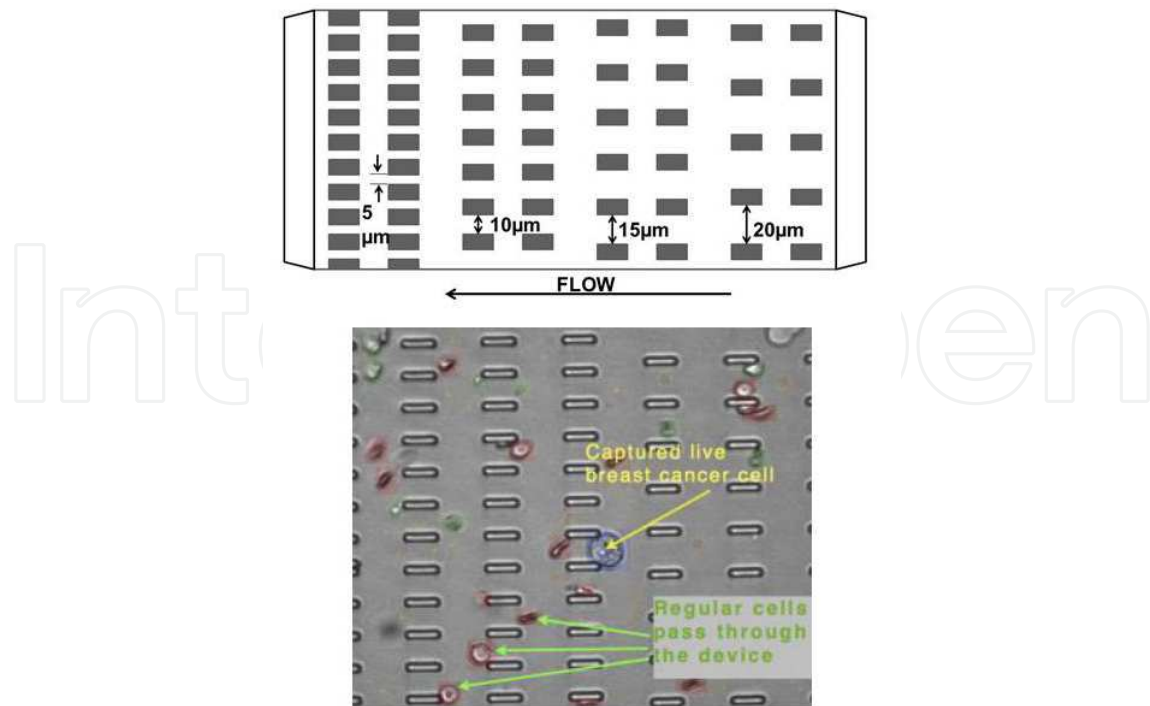


Figure 10. (top) Schematic showing flow direction and channel structure for the Second generation device having varying channel gap widths (20, 15, 10, and 5 μm), cells separate based on size and deformability. Channel depths, constant over a single device are: 20 or 10 μm . (Bottom) Adult blood cells spiked with MDA231 cells. All cells flow freely through the device except for the MDA231 cells, which are retained at the start of the 10 μm wide channels

A derivative of the same design was utilized to separate fetal cells from cord blood [91]. The device has four segments of successively narrower channels along the flow axis; these have 15, 10, 5, and 2.5 μm spacings. Each segment is 30 mm wide and 15 mm long and has 375 rows of channels of the same width. Therefore, the entire device is 30mm wide and 60mm long, giving rise to over 3.5 million channels. The channels are formed between pillars separated by gaps rather than a continuous structure. This design was favored to allow the cells to deform and resume their normal shape as they traverse the device; further, if the cell flow is locally slowed or if a channel becomes clogged, a cell is able to migrate around the affected area. Currently, a one-step centrifugation is required for sample preparation, and only the mononuclear layer is used in the device. This step not only separates most of the mature RBCs before sample loading, but it also enriches for fNRBCs since mononuclear cells and fNRBCs have similar densities. To identify fNRBCs, we stained the buffy coat with fluorescein isothiocyanate-labeled monoclonal antibody to HbF (green) and SYTO red. Thus, fNRBCs should fluoresce green and red. Double-stained samples were applied to the device. When the mononuclear layer was tested in the device, WBCs were retained consistently at the start of the 2.5 μm wide segment, while fNRBCs and mature RBCs migrated to the output reservoir. Cells were removed from the output reservoir, and the DNA was extracted with DNA purification kit and was tested for X and Y chromosomal sequence by PCR. We used cord blood from mothers who delivered male babies, so the X and Y chromosome could be used to demonstrate that the isolated cells

came from the baby and not the mother. Mature RBCs do not have a nucleus, and hence do not contaminate the DNA obtained [92].

5. Conclusion

In the last two decades, we witnessed many advances in microfluidic devices, and many of these devices are in advanced development stages or are commercially available. Microfluidic technology offers superior capability to precisely engineer and control the microenvironment to sort cells. Micro- and nano-fluidic technology will fulfill the sensitivity, specificity, and reproducibility requirements to bring cell sorting into clinical utility. The challenge remains to demonstrate that information acquired using microfluidic devices would change the way physicians diagnose, treat, and/or monitor diseases.

Author details

Hisham Mohamed

Egypt Nanotechnology Center (EGNC), Egypt

6. References

- [1] Fisher D, Francis GE. and Rickwood D. Cell Separation. New York: Oxford; 1998.
- [2] Wheeler AR, Thronset WR, Whelan RJ, Leach AM, Zare RN, Liao YH, Farrell K, Manger ID, Daridon A. Microfluidic Device for Single-Cell Analysis. *Anal. Chem.* 2003;75 (14) 3581–3586.
- [3] Horan PK, Wheelless LL. Quantitative single cell analysis and sorting *Science* 1977: (198) 149-157.
- [4] Dino Di Carlo DD, Lee LP. Dynamic Single-Cell Analysis for Quantitative Biology. *Anal. Chem.* 2006: 78 (23) 7918–7925
- [5] Anselmetti D. Single Cell Analysis. Hoboken: Wiley: 2009
- [6] Iorgulescu DG, Kiroff GK. Minimal residual marrow disease: detection and significance of isolated tumour cells in bone marrow. *ANZ J Surg.* 2001: (71) 365-376.
- [7] Engell HC. Cancer cells in the circulating blood. *Acta Chir. Scand.* 1955: (Suppl) (210), 1955.
- [8] Vlems F A, Wobbes T, Punt CJ, Van Muijen GN. Detection and clinical relevance of tumor cells in blood and bone marrow of patients with colorectal cancer. *Anticancer Res.* 2003: (23) 523-530.
- [9] Gomez FA. Biological Applications of Microfluidics. Hoboken:Wiley; 2008.
- [10] Kumar CS. Microfluidic Devices In Nanotechnology. Hoboken: Wiley; 2010.
- [11] Polla DL, Erdman AG, Robbins WP, Markus DT, Diaz-Diaz J, Rizq R, Nam Y, Brickner HT, Krulevitch P, Wang A. Microdevices in medicine. *Annual Review of Biomedical Engineering* 2000: (2) 552-572.

- [12] Chou C, Austin RH, Bakajin O, Tegenfeldt JO, Castelino JA, Chan SS, Cox EC, Craighead, H, Darnton N, Duke T, Han J, Turner S. Sorting biomolecules with microdevices.. *Electrophoresis* 2000: (21) 81-90.
- [13] Lee TMH, Hsing I, Lao AIK, Carles MC. A miniaturized DNA amplifier: its application in traditional chineses medicine. *Anal Chem*, 2000: (72) 4242-4247.
- [14] Simpson JL, Elias S. Isolating fetal cells from maternal blood: Advances in prenatal diagnosis through molecular technology. *JAMA* 1993: (270) 2357-2361.
- [15] McCormick RM, Nelson RJ, Alonso-Amigo MG, Benvegna DJ, Hooper HH. Microchannel electrophoretic separations of DNA in injection-molded plastic substrates. *Anal Chem*. 1997: (69) 2626-2630.
- [16] Lagally ET, Medintz I, Mathies RA. Single-molecule DNA amplification and analysis in an integrated microfluidic device. *Anal Chem*. 2001: (73) 565-570.
- [17] Koch M, Evans A, Brunnschweiler A. *Microfluidic Technology and Applications*. Hertfordshire: Research Studies Press LTD: 2000.
- [18] Saliterman SS. *BioMEMS and Medical Microdevices*. Bellingham: SPIE Press; 2006.
- [19] Bunn HF, Aster JC. *Pathophysiology of Blood Disorders*. Boston: McGrawy Hill: 2010.
- [20] Stuart M, Nagel R. Sickle-cell disease. *The Lancet* 2004: 364 (9442) 1343-1360
- [21] Schaeffer CW, Partin AW, Isaacs WB, Coffey DS, Isaacs JT. Molecular and cellular changes associated with the acquisition of metastatic ability by prostatic cancer cells. *Prostate* 1994: (25) 249-265.
- [22] Pienta KJ, Coffey DS. Nuclear-cytoskeletal interactions: evidence for physical connections between the nucleus and cell periphery and their alteration by transformation. *J Cell Biochem*. 1992: (49) 357-365.
- [23] Nickerson JA. Nuclear dreams: the malignant alteration of nuclear architecture. *J Cell Biochem*. 1998: (70) 172-180.
- [24] Pawlak G, Helfman D M. Cytoskeletal changes in cell transformation and tumorigenesis. *Curr Opin Genet Dev*. 2001: (11) 41-47.
- [25] Konety BR, Getzenberg RH. Nuclear structural proteins as biomarkers of cancer. *J Cell Biochem, Suppl* 1999: (32-33) 183-191.
- [26] Backman V, Wallace MB, Perelman LT, Arendt JT, Gurjar R, Muller MG, Zhang Q, Zonios G, Kline E, McGilligan JA, Shapshay S, Valdez T, Badizadegan K, Crawford JM, Fitzmaurice M, Kabani S, Levin HS, Seiler M, Dasari RR, Itzkan I, Van Dam J, Feld MS, McGillican T. Detection of preinvasive cancer cells. *Nature* 2000: (406) 35-36.
- [27] Zola H, Swart B, Banham A, Barry S, Beare A, Bensussan A, Boumsell L, D Buckley C, Bühring HJ, Clark G, Engel P, Fox D, Jin BQ, Macardle PJ, Malavasi F, Mason D, Stockinger H, Yang X. CD molecules 2006--human cell differentiation molecules. *J Immunol Methods* 2007: 318 (1-2) 1-5.
- [28] Went P, Lugli A., Meier S , Bundi M, Mirlacher M, Sauter G, Dirnhofer S. Frequent EpCam Protein Expression in Human Carcinomas. *Human Pathology* 2004: (35) 122-128.
- [29] Gastl G, Spizzo G, Obrist P, Dunser M, Mikuz G. Ep-CAM overexpression in breast cancer as a predictor of survival. *The Lancet* 2000: (356) 1981-1082.

- [30] Spizzo G, Gastl G, Wolf D, Gunsilius E, Steurer M, Fong D, Amberger A, Margreiter R, Obrist P. Correlation of COX-2 and Ep-CAM overexpression in human invasive breast cancer and its impact on survival. *Br J Cancer* 2003; (88) 574-587.
- [31] Spizzo G, Went P, Dirnhofer S, Obrist P, Simon R, Spichtin H, Maurer R, Metzger U, Castelberg B, Bart R, Stopatschinskaya S, Kochli O, Haas P, Mross F, Zuber M, Dietrich H, Bischoff S, Mirlacher M, Sauter G, Gastl G. High Ep-CAM expression is associated with poor prognosis in node positive breast cancer. *Breast Cancer Research and Treatment* 2004; (89) 207-213.
- [32] Talasz AH, Powell AA, Huber DE, Berbee JG, Roh KH, Yu W, Xiao W, Davis MM, Pease RF, Mindrinos MN, Jeffrey SS, Davic RW. Isolating highly enriched populations of circulating epithelial cells and other rare cells from blood using a magnetic sweeper device. *PNAS* 2009; (106) 10 3970-3975.
- [33] Kovacs GTA. *Micromachined Transducers Sourcebook*. Boston: McGraw Hill; 1998
- [34] Madou MJ. *Fundamentals of Microfabrication* 2nd edn. Boca Raton: CRC Press: 2002.
- [35] Coventor Inc. [Http://coventor.com/](http://coventor.com/) (accessed 29 April 2012).
- [36] ANSYS. [Http://ansys.com/](http://ansys.com/) (accessed 29 April 2012).
- [37] COMSOL. [Http://comsol.com/](http://comsol.com/) (accessed 29 April 2012).
- [38] Mohamed H, McCurdy LD, Szarowski DH, Duva S, Turner JN, Caggana M.
- [39] *IEEE Trans. NanoBio. Sci.* 2004; (3) 251-256.
- [40] Sin A, Murthy SK, Revzin A, Tompkins RG, Toner M. Enrichment Using Antibody-Coated Microfluidic Chambers in Shear Flow: Model Mixtures of Human Lymphocytes. *Biotechnology and Bioengineering* 2005; 91(7) 817-826.
- [41] Fu AY, Chou HP, Spence C, Arnold FH, Quake SR. An Integrated Microfabricated Cell Sorter. *Anal. Chem.* 2002; 74 (11) 2451-2457.
- [42] Revzin A, Sekine K, Sin A, Tompkins RG, Toner M. Development of a microfabricated cytometry platform for characterization and sorting of individual leukocytes. *Lab on a chip* 2005; (5) 30-37.
- [43] Chang WC, Lee LP, Liepmann D. Biomimetic technique for adhesion-based collection and separation of cells in a microfluidic channel. *Lab on a chip* 2005; (5) 64-73.
- [44] Madrusov E, Houg A, Klein E, Leonard EF. Membrane-based cell affinity chromatography to retrieve viable cells. *Biotechnol Prog* 1995; (11) 208-213
- [45] Malmstadt N, Yager P, Hoffman AS, Stayton PS. A Smart Microfluidic Affinity Chromatography Matrix Composed of Poly(*N*-isopropylacrylamide)-Coated Beads. *Anal. Chem* 2003; 75 (13) 2943-2949.
- [46] Kruger J, Singh K, O'Neill A, Jackson C, Morrison A, O'Brien P. Development of a microfluidic device for fluorescence activated cell sorting. *J. Micromech. Microeng.* 2002; (12) 486-494.
- [47] Dittrich PS, Schwille P. An Integrated Microfluidic System for Reaction, High-Sensitivity Detection, and Sorting of Fluorescent Cells and Particles. *Anal. Chem.* 2003; (75) 5767-5774.
- [48] Chung TD, Kim HC. Recent advances in miniaturized microfluidic flow cytometry for clinical use. *Electrophoresis* 2007; (28) 4511-4520.

- [49] Miyake R, Ohki H, Yamazaki I, Takagi T. Investigation of sheath flow chambers for flow cytometers (micromachined flow chamber with low pressure loss). *JSME Int. J. B* 1997; 40) 106–13.
- [50] Huh D, Gu W, Kamotani Y, Grotberg JB, Takayama S. Microfluidics for flow cytometric analysis of cells and particles. *Physiol. Meas.* 2005; (26) R73–R98.
- [51] Altendorf E, Zebert D, Holl M, Yager P. Differential blood cell counts obtained using a microchannel based flow cytometer. *Transducers 1997*: (97) 531–534.
- [52] Fu AY, Spence C, Scherer A, Arnold FH, Quake SR. A microfabricated fluorescence-activated cell sorter. *Nature Biotechnology* 1999; (17) 1109–1111
- [53] Oakey J, Allely J, Marr DWM. Laminar-Flow-Based Separations at the Microscale. *Biotechnol. Prog.* 2002; (18) 1439–1442.
- [54] Johansson L, Nikolajeff F, Johansson S, Thorslund S. On-Chip Fluorescence-Activated Cell Sorting by an Integrated Miniaturized Ultrasonic Transducer. *Anal. Chem.* 2009; (81) 5188–5196
- [55] Chun H, Chung TD, Kim HC, Cytometry and Velocimetry on a Microfluidic Chip Using Polyelectrolytic Salt Bridges. *Anal. Chem.* 2005; (77) 2490–2495.
- [56] Pamme N. Magnetism and microfluidics. *Lab on a chip* 2006; (6) 24–38.
- [57] Han KH, Frazier B. Paramagnetic capture mode magnetophoretic microseparator for high efficiency blood cell separations. *Lab on a Chip* 2006; (6) 265–273
- [58] Qu BY, Wu ZY, Fang F, Bai ZM, Yang DZ, Xu SK. A glass microfluidic chip for continuous blood cell sorting by a magnetic gradient without labeling. *Anal Bioanal Chem* 2008; (392) 1317–1324.
- [59] Adams JD, Kimb U, Sohb HT. Multitarget magnetic activated cell sorter. *PNAS* 2008; 105 (47) 18165–18170.
- [60] Xia N, Hunt TP, Mayers BT, Alsberg E, Whitesides GM, Westervelt RM, Ingber DE. Combined microfluidic-micromagnetic separation of living cells in continuous flow. *Biomed Microdevices* 2006; (8) 299–308.
- [61] Modak N, Datta A, Ganguly R. Cell separation in a microfluidic channel using magnetic microspheres. *Microfluid Nanofluid* 2009; (6) 647–660.
- [62] Lee H, Purdon AM, Westervelt RM. Manipulation of biological cells using a microelectromagnet matrix. *Applied Physics Letters* 2004; (85) 1063–1065.
- [63] Salibaa AE, Saiasa L, Psycharia E, Minca N, Simonb D, Bidardc FC, Mathiotd C, Piergac JY, Fraisierv V, Salamerof J, Saadag V, Faraceg F, Vielhg P, Malaquina L, Jean-Louis Viovy JL. Microfluidic sorting and multimodal typing of cancer cells in self-assembled magnetic arrays. *PNAS* 2010; (107) 33 14525–14529.
- [64] Kose AR, Koser H. Ferrofluid mediated nanocytometry. *Lab on a Chip* 2012; (12) 190–196.
- [65] Li, D *Electrokinetics in microfluidics*, 1st edition, vol. 2, Elsevier, Amsterdam (2004).
- [66] Al-Abboodi A, Tjeung R, Doran P, Yeo L, Friend J, Chan P. Microfluidic chip containing porous gradient for chemotaxis study. *Proc. of SPIE* 2011; (8204) H1–H6
- [67] Agrawal N, Toner M, Irimia D. Twelfth International Conference on Miniaturized Systems for Chemistry and Life Sciences: conference proceedings, October 12–16, 2008, San Diego, California, USA.

- [68] Chen YC, Lou X, Ingram P, Yoon E. The 15th International Conference on Miniaturized Systems for Chemistry and Life Sciences: conference proceedings, October 2-6, 2011, Seattle, Washington.
- [69] Englert DL, Manson MD, Jayaraman A. Flow-Based Microfluidic Device for Quantifying Bacterial Chemotaxis in Stable, Competing Gradients. *Applied and Environmental Microbiology* 2009: (75) 4557-4564
- [70] Walker GM, Sai J, Richmond A, Stremmer M, Chung CY, Wikswo JP. Effects of flow and diffusion on chemotaxis studies in a microfabricated gradient generator. *Lab on a Chip* 2005: (5) 611-618.
- [71] MacDonald MP, Spalding GC, Dholakia K. Microfluidic sorting in an optical lattice. *Nature* 2003: (426) 421-424.
- [72] Kovac JR, Voldman J. Intuitive, Image-Based Cell Sorting Using Optofluidic Cell Sorting. *Anal. Chem.* 2007: (79) 9321-9330.
- [73] Shirasaki Y, Tanaka J, Makazu H, Tashiro K, Shoji S, Tsukita S, Funatsu T. On-Chip Cell Sorting System Using Laser-Induced Heating of a Thermoreversible Gelatin Polymer to Control Flow. *Anal Chem* 2006: (78) 695-701.
- [74] Lin CC, Chen A, Kin CH. Microfluidic cells counter/sorter utilizing multiple particle tracing technique and optically switching approach. *Biomed Microdevices* 2008: (10) 55-63.
- [75] Hwang H, Park JK. Optoelectrofluidic platforms for chemistry and biology. *Lab on a Chip* 2011: (11) 33-47.
- [76] Wang MM, Tu E, Raymond DE, Yang MJ, Zhang H, Hagen N, Dees B, Mercer EM, Forster AH, Kariv I, Marchand PJ, Butler W. *Nature Biotechnology* 2004: (23) 83-87.
- [77] Pommer MS, Zhang Y, Keerthi N, Chen D, Thomson JA, Meinhard CD, Soh, HT. Dielectrophoretic separation of platelets from diluted whole blood in microfluidic channels. *Electrophoresis* 2008: (29) 1213-1218.
- [78] Hu X, Bessette PH, Qian J, Meinhard CD, Daugherty PS, Soh HT. Marker-specific sorting of rare cells using dielectrophoresis. *PNAS* 2005: (102) 44 15757-15761.
- [79] Vahey MD, Voldman J. An Equilibrium Method for Continuous-Flow Cell Sorting Using Dielectrophoresis. *Anal Chem* 2008: (80) 3135-3143.
- [80] Lapizco-Encinas BH, Simmons BA, Cummings EB, Fintschenko Y. Dielectrophoretic Concentration and Separation of Live and Dead Bacteria in an Array of Insulators. *Anal Chem* 2004: (76) 1571-1579.
- [81] Morijiri T, Sunahiro S, Senaha M, Yamada M, Seki M. Sedimentation pinched-flow fractionation for size- and density-based particle sorting in microchannels. *Microfluid Nanofluid* 2011: (11) 105-110.
- [82] Wilding P, Kricka LJ, Cheng J, Hvichia G, Shoffner MA, Fortina P. Integrated cell isolation and polymerase chain reaction analysis using silicon microfilter chambers. *Anal Biochem* 1998: (257) 95-200.
- [83] Yuen PK, Kricka LJ, Fortina P, Panaro PJ, Sakazume T, Wilding P. Microchip module for blood sample preparation and nucleic acid amplification reactions. *Genome Res* 2001: (11) 405-412.

- [84] Panaro NJ, Lou XJ, Fortina P, Kicka LJ, Wilding P. Micropillar array chip for integrated white blood cell isolation and PCR. *Biomed Eng* 2005: (21) 157-162.
- [85] Cabodi M, Chen YF, Turner SWP, Craighead HG, Austin RH. Continuous separation of biomolecules by the laterally asymmetric diffusion array with out-of-plane sample injection. *Electrophoresis* 2002: (23) 3496–3503.
- [86] Huang LR, Cox EC, Austin RH, Sturm JC. Continuous Particle Separation Through Deterministic Lateral Displacement. *Science* 2004: (304) 987-990.
- [87] Davis JA, Inglis DW, Morton KJ, Lawrence DA, Huang LR, Chou SY, Sturm JC, Austin RH. Deterministic hydrodynamics: Taking blood apart. *PNAS* 2006: 103 (40) 14779–14784.
- [88] Mohamed H, McCurdy LD, Szarowski DH, Duva S, Turner JN, Caggana M. Development of a Rare-Cell Fractionation Device: Application for Cancer Detection. *IEEE Transactions on NanoBioscience* 2004: (3) 251-256.
- [89] H. Mohamed, M. Murray, J. N. Turner, and M. Caggana, "Circulating tumor cells: capture with a micromachined device," *Proceedings of the 2005 NSTI Bio Nano Conference*, vol1, pp. 1-4, 2005.
- [90] Mohamed H, Murray M, Turner JN, Caggana M. Isolation of tumor cells using size and deformation. *Journal of Chromatography A* 2009: (1216) 8289–8295.
- [91] H. Mohamed, J. N. Turner, and M. Caggana. *Bio Nano Conference: conference proceedings*, May 7-11, 2006, Hynes Convention Center, Boston Massachusetts.
- [92] Mohamed H, Turner JN, Caggana M. *Bio Nano Conference: conference proceedings*, May 20-24, 2007, Santa Clara, California.
- [93] Murthy SK, Sethu P, Vunjak-Novakovic G, Toner M, Radisic M. Size-based microfluidic enrichment of neonatal rat cardiac cell populations. *Biomed Microdevices* 2006: (8) 231–237.
- [94] Huang R, Barber TA, Schmidt MA, Tompkins RG, Toner M, Bianchi DW, Kapur R, Flejter WL. A microfluidics approach for the isolation of nucleated red blood cells (fNRBCs) from the peripheral blood of pregnant women. *Prenat Diagn.* 2008: (28) 892–899.